Myt1 protein kinase is essential for Golgi and ER assembly during mitotic exit

Hiroyuki Nakajima,[1] Shigenobu Yonemura,[2] Masayuki Murata,[3] Nobuhiro Nakamura,[4] Helen Piwnica-Worms,[5,6] and Eisuke Nishida[1]

[1]Department of Cell and Developmental Biology, Graduate School of Biostudies, Kyoto University, Sakyo-ku, Kyoto 606-8502, Japan
[2]Laboratory for Cellular Morphogenesis, RIKEN Center for Developmental Biology, Kobe 650-0047, Japan
[3]Department of Life Sciences, Graduate School of Arts and Sciences, University of Tokyo, Tokyo 153-8902, Japan
[4]Division of Life Sciences, Graduate School of Natural Science and Technology, Kanazawa University, Kakuma, Kanazawa 920-1192, Japan
[5]Department of Cell Biology and Physiology and [6]Department of Internal Medicine, Howard Hughes Medical Institute, Washington University School of Medicine, St. Louis, MO 63110

Myt1 was originally identified as an inhibitory kinase for Cdc2 (Cdk1), the master engine of mitosis, and has been thought to function, together with Wee1, as a negative regulator of mitotic entry. In this study, we report an unexpected finding that Myt1 is essential for Golgi and endoplasmic reticulum (ER) assembly during telophase in mammalian cells. Our analyses reveal that both cyclin B1 and cyclin B2 serve as targets of Myt1 for proper Golgi and ER assembly to occur. Thus, our results show that Myt1-mediated suppression of Cdc2 activity is not indispensable for the regulation of a broad range of mitotic events but is specifically required for the control of intracellular membrane dynamics during mitosis.

Introduction

Activation of Cdc2 and its translocation to the nucleus are the crucial events controlling entry into mitosis (Nurse, 1990; Hunt, 1991; Pines, 1999; Takizawa and Morgan, 2000). In multicellular eukaryotes, the kinase activity of Cdc2 is generally considered to be regulated by inhibitory phosphorylation on Thr14 and Tyr15, which are catalyzed by Wee1 and Myt1 (Lew and Kornbluth, 1996; Nigg, 2001). Wee1, which was identified originally in a *Schizosaccharomyces pombe* mutant with a small cell or wee phenotype, is a tyrosine-specific protein kinase conserved in all eukaryotes. Human Wee1 is nuclear and phosphorylates Cdc2 exclusively on Tyr15 (Parker and Piwnica-Worms, 1992; Heald et al., 1993; McGowan and Russell, 1993; Parker et al., 1995). Myt1, a membrane-associated kinase, is present in metazoans and phosphorylates Cdc2 on both Thr14 and Tyr15 residues (Kornbluth et al., 1994; Mueller et al., 1995; Booher et al., 1997; Liu et al., 1997, 1999; Wells et al., 1999; Okumura et al., 2002). Thus, both Myt1 and Wee1 have been thought to function as negative regulators of mitotic entry.

In several known species, Myt1 but not Wee1 is present in immature oocytes and mediates prophase I arrest by inhibiting Cdc2 (Nakajo et al., 2000; Okumura et al., 2002). In *Xenopus laevis* oocytes, injection of neutralizing anti-Myt1 antibodies induces germinal vesicle breakdown, presumably through the activation of Cdc2 (Nakajo et al., 2000). In *Caenorhabditis*

elegans hermaphrodites, Myt1 depletion using RNAi has been shown to cause precocious maturation of oocytes (Burrows et al., 2006). Mutations in Myt1 in *C. elegans* also implicate its role in the regulation of male meiosis (Lamitina and L'Hernault, 2002). Furthermore, *Drosophila melanogaster* Myt1 has been shown to be important for the regulation of both mitotic and meiotic cell cycles during gametogenesis (Jin et al., 2005). More proliferating cells were observed in null *myt1* mutant testes and ovaries than in controls, and male *myt1* mutants show complete sterility. In addition, the loss of Myt1 causes elevated nondisjunction in homologous chromosome segregation during female meiosis I (Jin et al., 2005). Thus, Myt1 has a pivotal role in gametogenesis in various species. However, it is not known whether Myt1 functions to regulate mitotic entry during somatic cell cycles in vertebrates.

In this study, we examine the role of Myt1 in mammalian somatic cell cycles. Our results show that although the inhibition of Wee1 expression by siRNA markedly accelerates mitotic entry, inhibition of Myt1 expression does not change the timing of mitotic entry. Interestingly, our analysis demonstrates that Myt1 depletion induces severe defects in Golgi and ER assembly during mitotic exit. Thus, Myt1 is essential for Golgi and ER assembly at the end of mitosis. Furthermore, cyclin B1 and B2 knockdown experiments demonstrate that Myt1 functions to facilitate Golgi and ER assembly through its ability to suppress both cyclin B1– and cyclin B2–Cdc2 activities. Thus, our findings have identified

Correspondence to Eisuke Nishida: L50174@sakura.kudpc.kyoto-u.ac.jp

Myt1 as an essential regulator of intracellular membrane dynamics during mitosis in mammalian somatic cell cycles.

Results

The effects of Myt1 and Wee1 siRNAs on the timing of mitotic entry in HeLa cells

To determine whether human Myt1 levels vary throughout the somatic cell cycle, we examined Myt1 protein levels in synchronized HeLa cells. Myt1 levels peaked at M phase, at 9–11 h after release from a thymidine block, and markedly decreased after M phase (Fig. 1 A, top left). In contrast to cyclin B1, whose protein levels peaked at 9 h and dropped rapidly, Myt1 protein levels remained high at 10–11 h, indicating that Myt1 is present at relatively high levels during M phase even after the metaphase-anaphase

transition. As previously reported, the mobility of Myt1 is reduced on SDS gels as a result of phosphorylation during M phase (Mueller et al., 1995; Booher et al., 1997; Liu et al., 1997, 1999; Wells et al., 1999; Okumura et al., 2002). To exclude the possibility that the antibody used might recognize slower migrating forms of Myt1 more strongly, we examined Myt1 protein levels after treating cell extracts with λ phosphatase. The result also shows that Myt1 protein levels increase during M phase (Fig. 1 A, top right). Moreover, the decrease of Myt1 observed after M phase was markedly suppressed by treatment with MG132, a proteasome inhibitor (Fig. 1 A, bottom right), indicating that Myt1 degradation directly or indirectly requires the ubiquitin-proteasome system at the end of M phase or during G1 phase.

To examine the role of Myt1 in mitotic entry in somatic cell cycles, siRNA was used to reduce Myt1 levels in synchronized
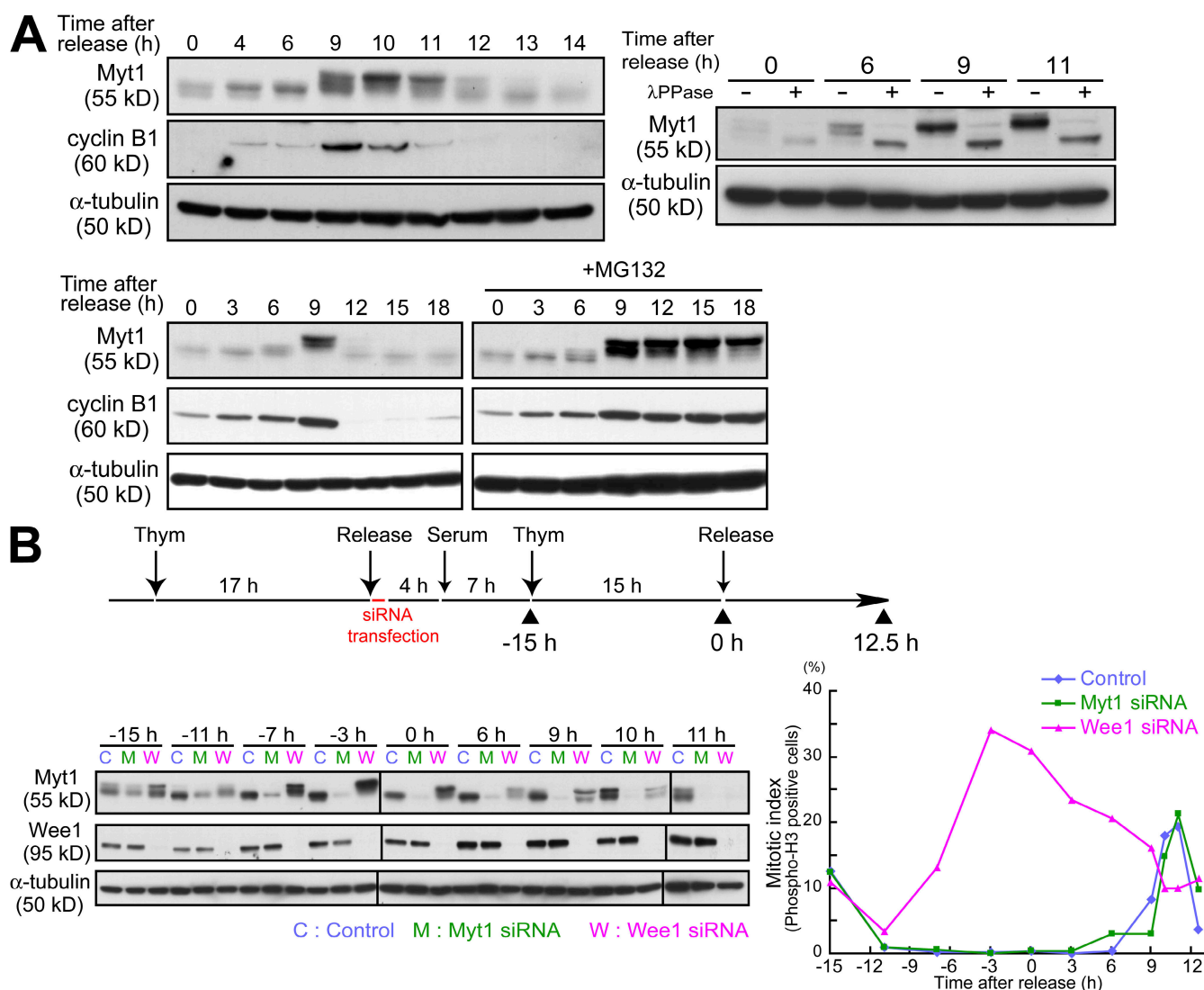

Figure 1. **The effect of Myt1 and Wee1 siRNAs on the timing of mitotic entry in HeLa cells.** (A) Extracts were prepared from HeLa cells synchronized by a double-thymidine block and analyzed by SDS-PAGE followed by immunoblotting with anti-Myt1, anti–cyclin B1, and anti–α-tubulin antibodies (top and bottom left). MG132 was added to synchronized cells 8 h after release (bottom right). Extracts from synchronized cells were treated with or without λ protein phosphatase and were subjected to immunoblotting with anti-Myt1 and anti–α-tubulin antibodies (top right). (B) HeLa cells were transfected with Myt1 or Wee1 siRNA in the interval between the two thymidine blocks (top; experimental protocol). Cell extracts were analyzed by SDS-PAGE followed by immunoblotting with anti-Myt1, anti-Wee1, and anti–α-tubulin antibodies (bottom left). The cells were examined for the percentage of mitotic cells using antiphosphohistone H3 antibody (bottom right). More than 300 cells were examined, and the percentages are shown as mitotic index.

HeLa cells. HeLa cells were transfected with Myt1 siRNA during the interval between the two thymidine blocks (Fig. 1 B, top). The percentage of mitotic cells was determined using a phosphohistone H3 antibody that specifically detects mitotic cells. The effect of Wee1 siRNA on the timing of mitotic entry was also examined. In untreated control cells, the percentage of the mitotic cells peaked at 10 h after release from the G1/S block (Fig. 1 B). The Myt1 siRNA-treated cells showed almost the same time course of mitotic entry as the control cells, whereas the Wee1 siRNA-treated cells entered mitosis much earlier than the control and Myt1 siRNA-treated cells (Fig. 1 B). Essentially the same results were obtained in another series of experiments in which MPM2-positive cells or condensed chromosomes were used as the mitotic indices (unpublished data). These results suggest that Myt1, unlike Wee1, may be less important for regulating mitotic entry timing in HeLa cells.

Myt1 is necessary for Golgi reassembly during telophase

In Myt1 siRNA-treated cells, a mitotic spindle was formed normally, and interphase microtubules emanated from centrosomes normally and extended toward the cell periphery, although they appeared to be slightly less dense (Fig. 2 A). In these cells, the number and size of centrosomes were also apparently normal, and

the actin cytoskeleton and lysosomes were indistinguishable from those in control cells (Fig. 2 B). The Golgi apparatus, however, displayed a dramatically transformed morphology in Myt1-depleted cells. Immunofluorescence staining for Golgi matrix proteins GM130 and p115 revealed markedly condensed non-ribbon-like membranous structures near the nucleus, which are clearly different from normal Golgi structures in control cells (Fig. 3 A) and control siRNA-treated cells (not depicted). Immunofluorescence staining for other Golgi markers, including v-SNARE GS15, t-SNARE Vti1a, and Golgin-245/p230, revealed similar differences in the staining patterns between Myt1-depleted cells and control cells (unpublished data). Furthermore, most ER exit sites localized around such Golgi marker–positive condensed structures (Fig. 3 C). Interestingly, γ-adaptin, which localizes to the TGN in control cells, rarely associated with these abnormal membranous structures in Myt1-depleted cells but rather was dispersed throughout the cytoplasm (Fig. 3 B). In Myt1-depleted cells, the other TGN markers, Golgin97 and TGN38, were not dispersed but associated with the condensed membranous structures like other cis- and medial-Golgi markers (Fig. 3 B and not depicted). As γ-adaptin is a clathrin adaptor and functions to facilitate transport from the TGN to both endosomes and the plasma membrane, Myt1-depleted cells may be deficient in these transporting abilities. A portion of Myt1-depleted cells displayed large
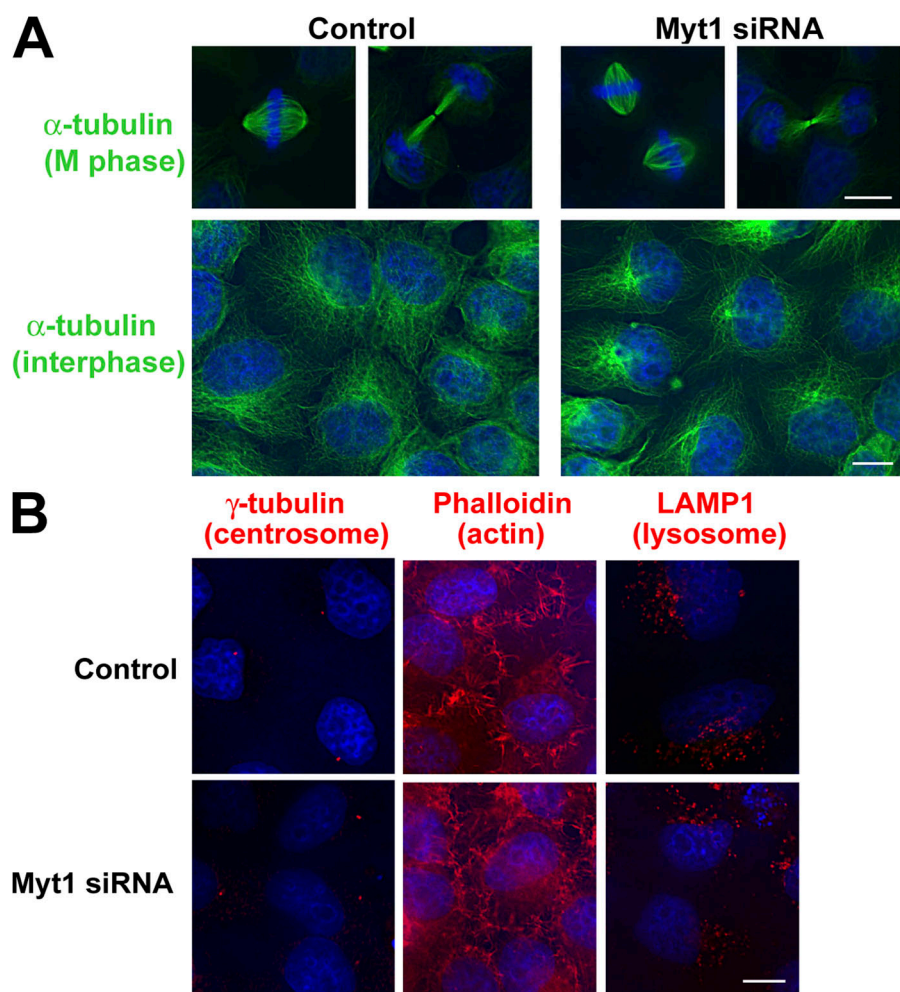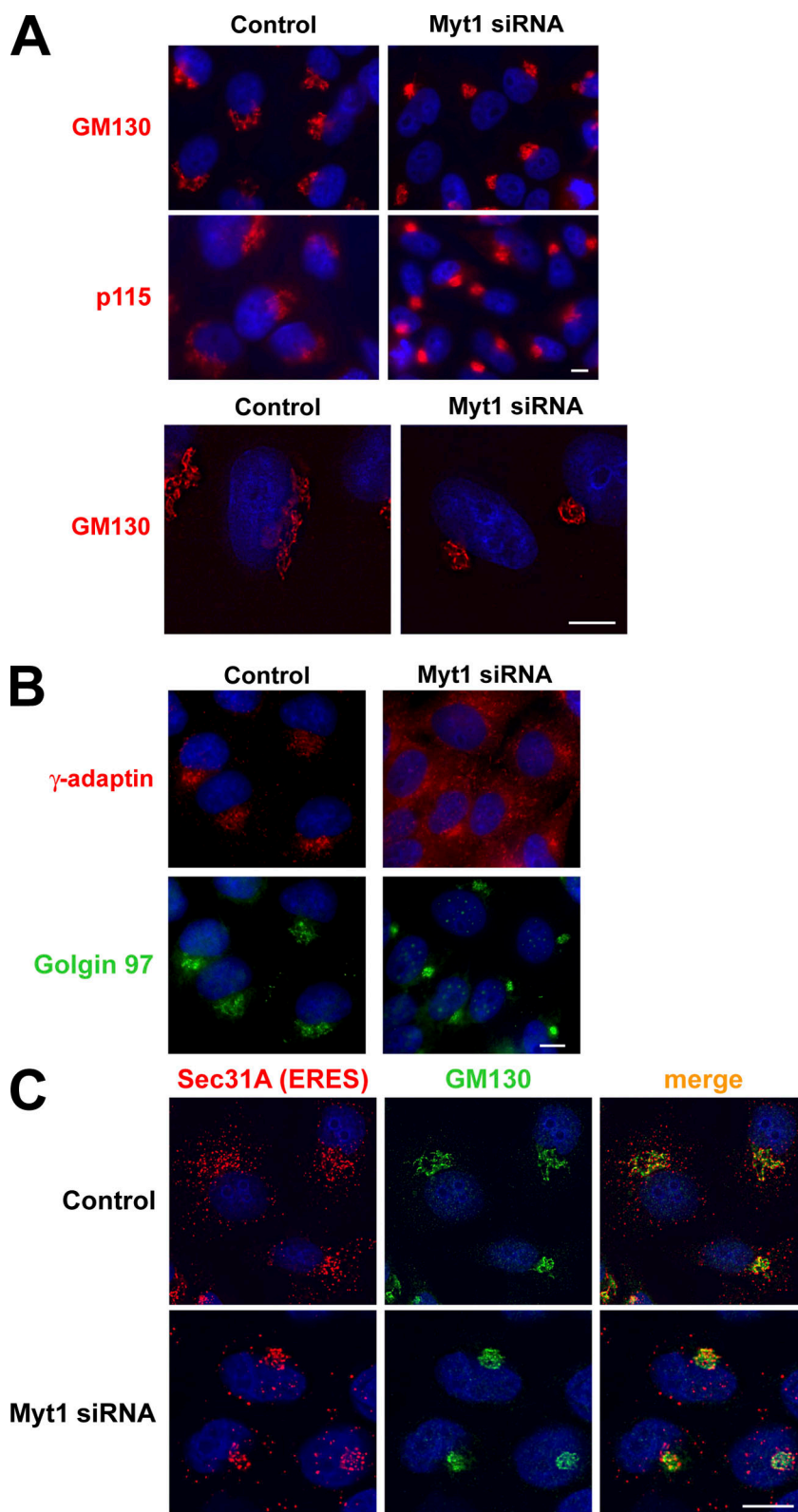
Figure 2. **Effect of Myt1 depletion on cytoskeleton and subcellular organelles.** HeLa cells were transfected with Myt1 siRNA and incubated for 48 h. (A) M-phase (top) and interphase (bottom) cells were stained with anti–α-tubulin antibody (green) together with Hoechst (blue). (B) Cells were stained with anti–γ-tubulin antibody for centrosomes (left), fluorescent phalloidin for actin cytoskeleton (middle), and anti-LAMP1 antibody for lysosomes (right; red) together with Hoechst (blue). Bars, 10 μm.

Figure 3. **Depletion of Myt1 induces dramatic changes in the Golgi apparatus and ER exit sites.** HeLa cells were transfected with Myt1 siRNA and incubated for 48 h. (A) The cells were stained with anti-GM130 and anti-p115 antibodies (red) together with Hoechst (blue). High resolution images (GM130) were obtained by deconvolution (bottom). (B) The cells were stained with anti–γ-adaptin antibody (red) together with anti–Golgin97 antibody (green) and Hoechst (blue). (C) The cells were stained with anti-Sec31A antibody (red) for ER exit sites together with anti-GM130 antibody (green) and Hoechst (blue). Bars, 10 µm.

vacuoles (unpublished data), which may be the result of transport defects. Moreover, we found that Myt1-depleted cells showed a retarded proliferation rate and died within 10 d. Thus, Myt1 is likely to be essential for Golgi structure and function.

Myt1 might function to maintain Golgi structure during interphase, or, alternatively, Myt1 might be essential for Golgi reassembly during mitotic exit. The Golgi apparatus fragments into thousands of vesicles and tubules during prometaphase and rapidly reassembles during telophase in mammalian cells (Shorter and Warren, 2002). To distinguish between these two possibilities, we transfected synchronized HeLa cells with Myt1 siRNA as in Fig. 1 B and stained the cells with anti-GM130 antibody
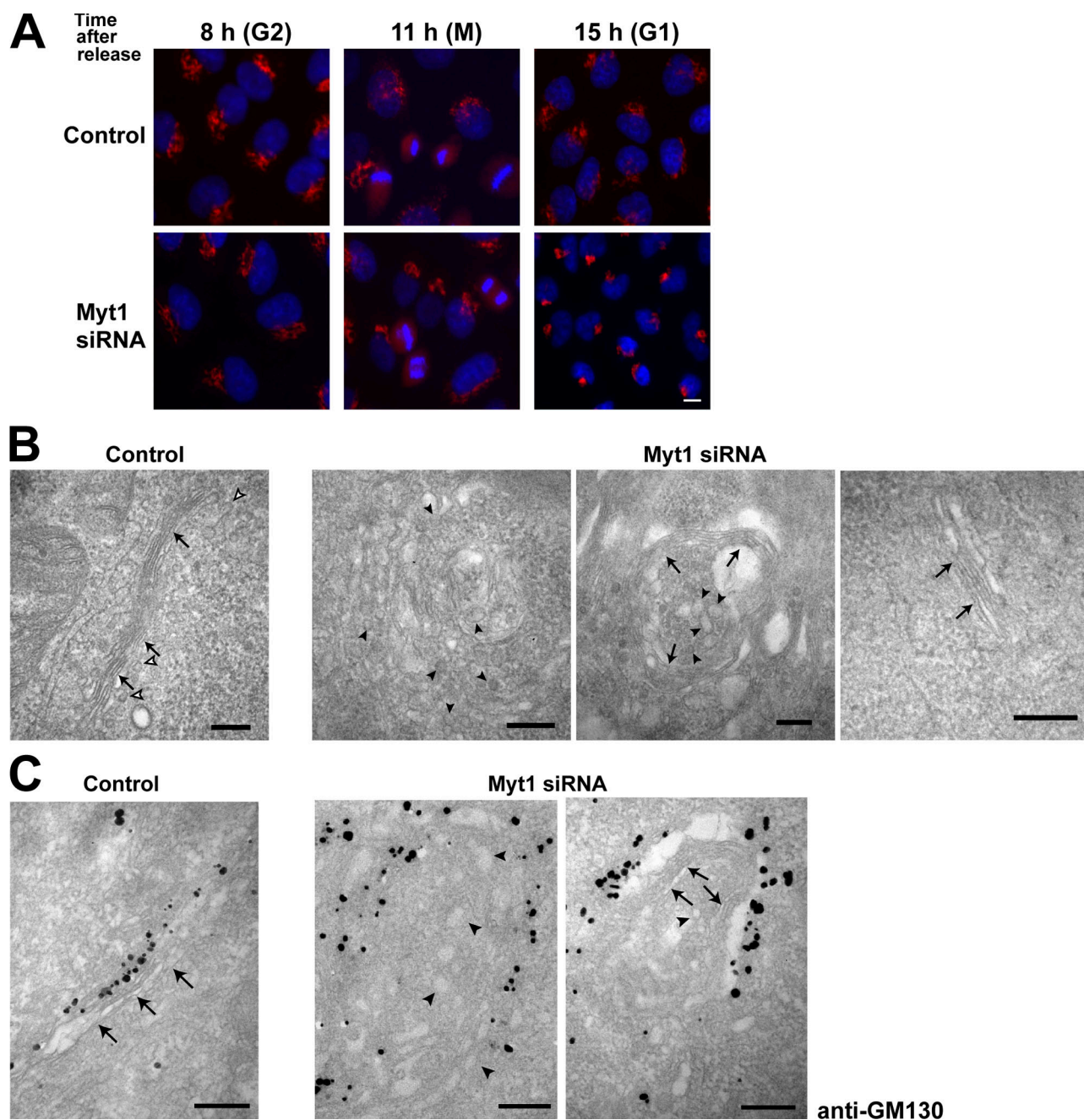
Figure 4. **Myt1 is required for Golgi reassembly during telophase.** (A) Synchronized HeLa cells were transfected with Myt1 siRNA as in Fig. 1 B, and cells at 8 (G2), 11 (M), and 15 h (G1) after the release were stained with anti-GM130 antibody (red) and Hoechst (blue). (B) Representative electron microscopy images of Golgi in cells that were transfected with or without Myt1 siRNA and incubated for 48 h. (C) Immunolabeling electron microscopy images of the Golgi area in HeLa cells transfected with or without Myt1 siRNA. For immunolabeling of Golgi marker proteins, monoclonal antibody to GM130 was used. (B and C) Arrows show cisternae or long tubules. White arrowheads show transport vesicles, and black arrowheads show short tubules and vesicles. Bars: (A) 10 μm; (B and C) 0.2 μm.

as cells progressed through the cell cycle after release from the G1/S block. In G2 phase, Myt1-depleted cells had normal ribbon-like Golgi structures (Fig. 4 A, 8 h) in spite of the complete loss of Myt1 (Fig. 1 B). Also, the Golgi fragmentation occurred normally during prometaphase in Myt1-depleted cells (Fig. 4 A, 11 h). However, in G1 phase after mitosis, the staining pattern showed abnormal, markedly condensed, nonribbon-like membranous structures (Fig. 4 A, 15 h). Thus, Myt1 depletion induced severe defects in Golgi reassembly. We confirmed that such a

phenotype persisted through G1 into S and G2 phases (unpublished data). We have also revealed that Golgi restoration after brefeldin A washout in Myt1-depleted cells was normal and not delayed compared with the restoration in control cells (unpublished data). These results have clearly shown that Myt1 is required for Golgi reassembly during telophase but not for the maintenance of Golgi structure during interphase.

Electron microscopy was used to examine the morphology of the Golgi apparatus in Myt1-depleted cells. Although the
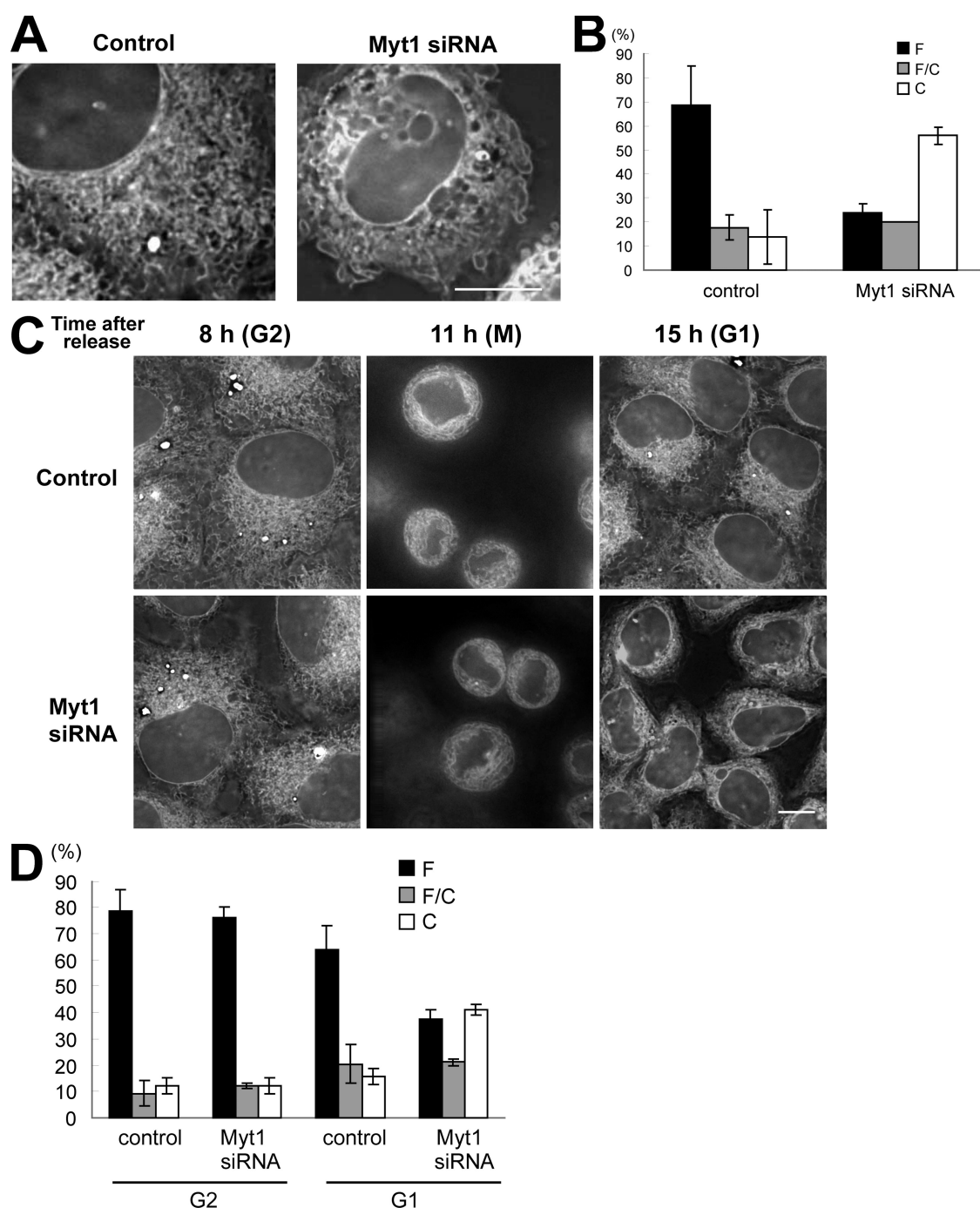
A Control   Myt1 siRNA

B (%)

C Time after release   8 h (G2)   11 h (M)   15 h (G1)

Control

Myt1 siRNA

D (%)

Figure 5. **Myt1 is required for ER meshwork formation.** (A) HeLa cells were transfected with Myt1 siRNA and incubated for 48 h. The ER was visualized with ER tracker red in living cells without fixation. (B) The cells in A were classified into three types based on the ER morphology. The cells that have a fine ER meshwork consisting of typical tubular structures throughout the cytoplasm were classified into a fine meshwork type (labeled as F). The cells that have a coarse ER meshwork and thick, cisternae-like structures in the cell periphery were classified into a coarse meshwork type (labeled as C). The cells that show intermediate phenotypes were classified into a fine/coarse meshwork type (labeled as F/C). More than 40 cells were examined. The bars are the mean of two independent experiments. (C) Synchronized HeLa cells were transfected with Myt1 siRNA as in Fig. 1 B, and ER was visualized with ER tracker red in living cells at 8 (G2), 11 (M), and 15 h (G1) after the release. (D) The G2 and G1 cells in C are classified into three types based on the ER morphology. More than 45 cells were examined in each experiment, and experiments were performed twice. (B and D) Error bars represent ±SD. Bars, 10 μm.

normally stacked Golgi cisternae could be observed in more than three fourths of control cells (Fig. 4 B, control), stacked Golgi-like cisternae could be detected only in approximately one third of Myt1 siRNA-treated cells. Moreover, the stacked Golgi-like cisternae in Myt1-depleted cells were loosely stacked and abnormal in appearance (Fig. 4 B, Myt1 siRNA; right). Two types of aberrant membranous structures were observed exclusively in Myt1-depleted cells (Fig. 4 B, Myt1 siRNA; left and middle). These included structures composed of short tubules and an abundance of vesicles (Fig. 4 B, Myt1 siRNA; left),

which were likely derived from mitotic Golgi fragments, and condensed structures consisting of vesicles surrounded by abnormally bended stacks of long tubules (Fig. 4 B, Myt1 siRNA; middle). Immunoelectron microscopy using an anti-GM130 antibody (Fig. 4 C) revealed that the abnormal membranous structures were derived from Golgi fragments and may correspond to the condensed nonribbon-like membranous structures seen with immunofluorescence staining (Fig. 3 A). Thus, the electron microscopy data support the conclusion that Myt1 functions to facilitate Golgi reassembly during telophase.

Myt1 is necessary for ER meshwork formation during telophase

Golgi is closely related to the ER (Lippincott-Schwartz et al., 2000). The ER is a continuous membrane system enclosing a single luminal space and comprises fine tubular networks and cisternae throughout the cytoplasm (Voeltz et al., 2002; Shibata et al., 2006). ER tracker labeling in live cells revealed that a fine ER meshwork became disrupted in Myt1 siRNA-treated cells; the meshwork of tubular structures became coarse, and thick, cisternae-like structures appeared in the cell periphery in Myt1-depleted cells (Fig. 5 A). To semiquantify this phenotype, the cells were classified into three types based on the ER morphology. The cells that had a fine ER meshwork consisting of typical tubular structures throughout the cytoplasm were classified into a fine meshwork type (Fig. 5 B, bars labeled F). The cells that had a coarse ER meshwork and thick, cisternae-like structures in the cell periphery were classified into a coarse meshwork type (Fig. 5 B, bars labeled with C). The cells that show intermediate phenotypes were classified into a fine/coarse meshwork type (Fig. 5 B, bars labeled with F/C). The semiquantification data in Fig. 5 B clearly show that Myt1 depletion induces disruption of a fine ER meshwork. When synchronized HeLa cells were transfected with Myt1 siRNA as in Fig. 1 B, Myt1-depleted cells had a normal, fine ER meshwork in G2 phase (Fig. 5, C and D; 8 h [G2]) in spite of the complete loss of Myt1 (Fig. 1 B), and, during mitosis, the ER morphology in Myt1-depleted cells was indistinguishable from that in control cells (Fig. 5 C, 11 h). However, in G1 phase after mitosis, ER tracker labeling showed an abnormal coarse meshwork of ER (Fig. 5, C and D; 15 h [G1]). Thus, Myt1 depletion induced severe defects in reassembly of a fine ER meshwork. Therefore, Myt1 is required for reassembly of a fine, interphase-type ER meshwork during mitotic exit but not for biogenesis or maintenance of an ER meshwork during interphase.

Kinase activity of Myt1 is necessary for Golgi and ER reassembly

To ensure that Myt1 siRNA specifically depletes cells of Myt1, we performed add-back experiments in synchronized HeLa cells. Expression of an siRNA-resistant form of Myt1 almost completely rescued the Golgi reassembly defect (Fig. 6 A, Myt1 siRNA + Myt1-WT; arrows). In contrast, expression of the siRNA-resistant form of Myt1 that lacks kinase activity did not rescue the phenotype (Fig. 6 A, Myt1 siRNA + Myt1-KD). To semiquantify the Golgi defect, GM130-stained images were
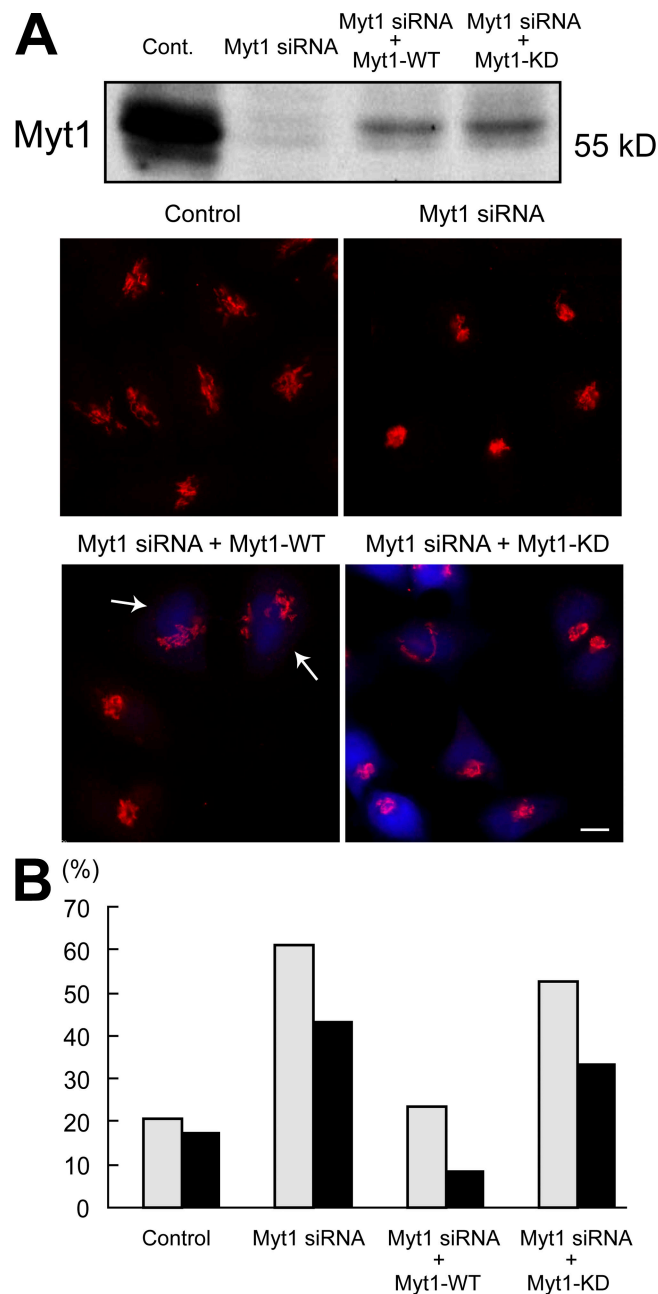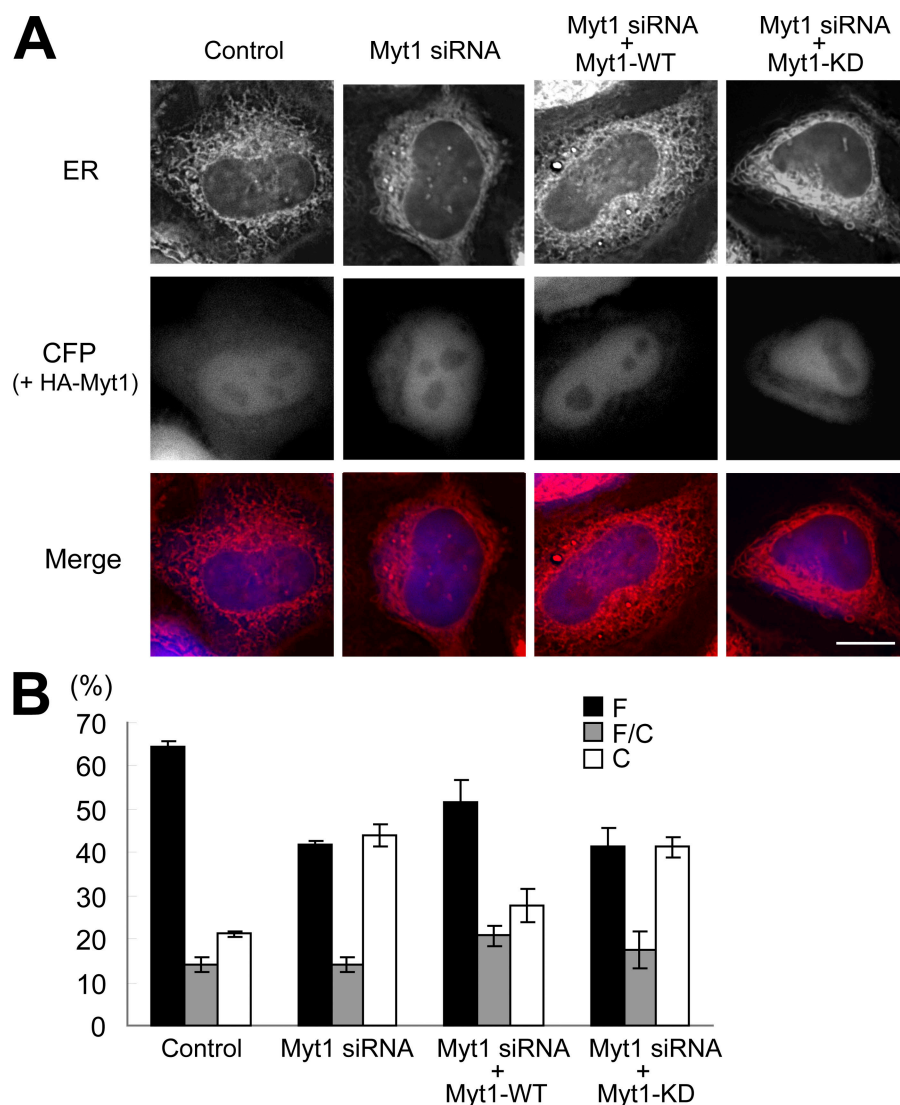

Figure 6. **Kinase activity of Myt1 is necessary for Golgi reassembly.** (A) HeLa cells were transfected with or without Myt1-WT or Myt1-KD (a kinase-inactive form of Myt1), which is resistant to Myt1 siRNA, together with CFP as an indicator of Myt1-expressing cells before the first thymidine block, and then Myt1 siRNA treatment was performed after the first thymidine block. 15 h after the release from G1/S block, cells were subjected to immunoblotting with anti-Myt1 antibody (top) or were fixed and stained with anti-GM130 antibody (red; bottom). Exogenous Myt1 levels in Myt1-depleted cells were lower than endogenous Myt1 levels in control cells (top). We confirmed that this level of Myt1 expression did not inhibit entry into mitosis (not depicted). Exogenous Myt1 was expressed only in CFP-positive cells (blue; bottom), and the Golgi reassembly defect was completely rescued by the expression of Myt1-WT (bottom left; arrows). (B) The relative Golgi area in anti-GM130 images in the cells described in A were measured (see Materials and methods). The percentage of cells whose Golgi area was smaller than one SD from the mean Golgi area of control cells was determined. More than 200 cells were examined in each experiment, and experiments were performed twice. The results obtained from each independent experiment are represented as distinct bars (gray and black bars for each experiment). Bar, 10 μm.

Figure 7. **Kinase activity of Myt1 is necessary for ER reassembly.** (A) HeLa cells were transfected with or without Myt1-WT or Myt1-KD, which is resistant to Myt1 siRNA, together with CFP as an indicator of Myt1-expressing cells before the first thymidine block, and then Myt1 siRNA treatment was performed after the first thymidine block. ER was visualized with ER tracker red in living cells 15 h after the release. (B) CFP-positive cells in A were classified into three types based on the ER morphology as described in Fig. 5 B. More than 32 cells were examined in each experiment, and experiments were performed twice or more. The bars are the mean of more than two independent experiments. Error bars represent ±SD. F, fine meshwork type; C, coarse meshwork type; F/C, fine/coarse meshwork type. Bar, 10 μm.

used to measure the Golgi area in Myt1-depleted and -restored cells. 19% of control cells and 52% of Myt1-depleted cells had a Golgi area smaller than one SD from the mean measured in control cells (Fig. 6 B). Expression of Myt1 in Myt1-depleted cells reduced the percentage of small, compact Golgi from 52 to 16% (Fig. 6 B), indicating an almost complete rescue of the phenotype. Expression of kinase-inactive Myt1 was unable to restore the integrity of the Golgi (43% of control; Fig. 6 B). These results demonstrate that the kinase activity of Myt1 is required for Golgi reassembly.

The Myt1 add-back experiments were also performed to examine the ER morphology in synchronized HeLa cells. When the siRNA-resistant form of Myt1 was expressed in Myt1 siRNA-treated cells, the ER reassembly defect, that is, the defect in reassembly of an interphase-type ER meshwork during telophase, was mostly rescued, and a fine ER meshwork appeared (Fig. 7, A and B; Myt1 siRNA + Myt1-WT). In contrast, expression of the siRNA-resistant form of Myt1 that lacks kinase activity did not rescue the ER reassembly defect (Fig. 7, A and B; Myt1 siRNA + Myt1-KD). Thus, the kinase activity of Myt1 is also required for ER reassembly.

Myt1 functions to facilitate Golgi and ER assembly through both cyclin B1 and cyclin B2

Cdc2 is the only known substrate of Myt1 (Booher et al., 1997). Cdc2 is bound to mitotic B-type cyclins and is then activated to form M phase–promoting factor (Nurse, 1990; Hunt, 1991). There are three mammalian B-type cyclins: cyclin B1, B2, and B3. Among these B-type cyclins, mammalian cyclin B3 is thought to be a meiosis-specific cyclin because it is detected in both the testis and ovary but not in any other tissues. The mRNA and the protein of human cyclin B3 could not be detected in HeLa cells (Nguyen et al., 2002). In contrast, cyclin B1 and cyclin B2 are ubiquitously present in somatic cells, and both protein levels peak at M phase (Pines, 1999). In our analysis in synchronized HeLa cells, cyclin B1 was mostly degraded during metaphase and anaphase (at ∼10 h after release in this series of experiments) as previously reported (Clute and Pines, 1999), but the protein appeared to be present at very low levels even in late mitosis (at ∼11–12 h; Fig. 8 A). In the same series of experiments, cyclin B2 was also mostly degraded after metaphase, but low levels, which were slightly higher than cyclin B1 levels,
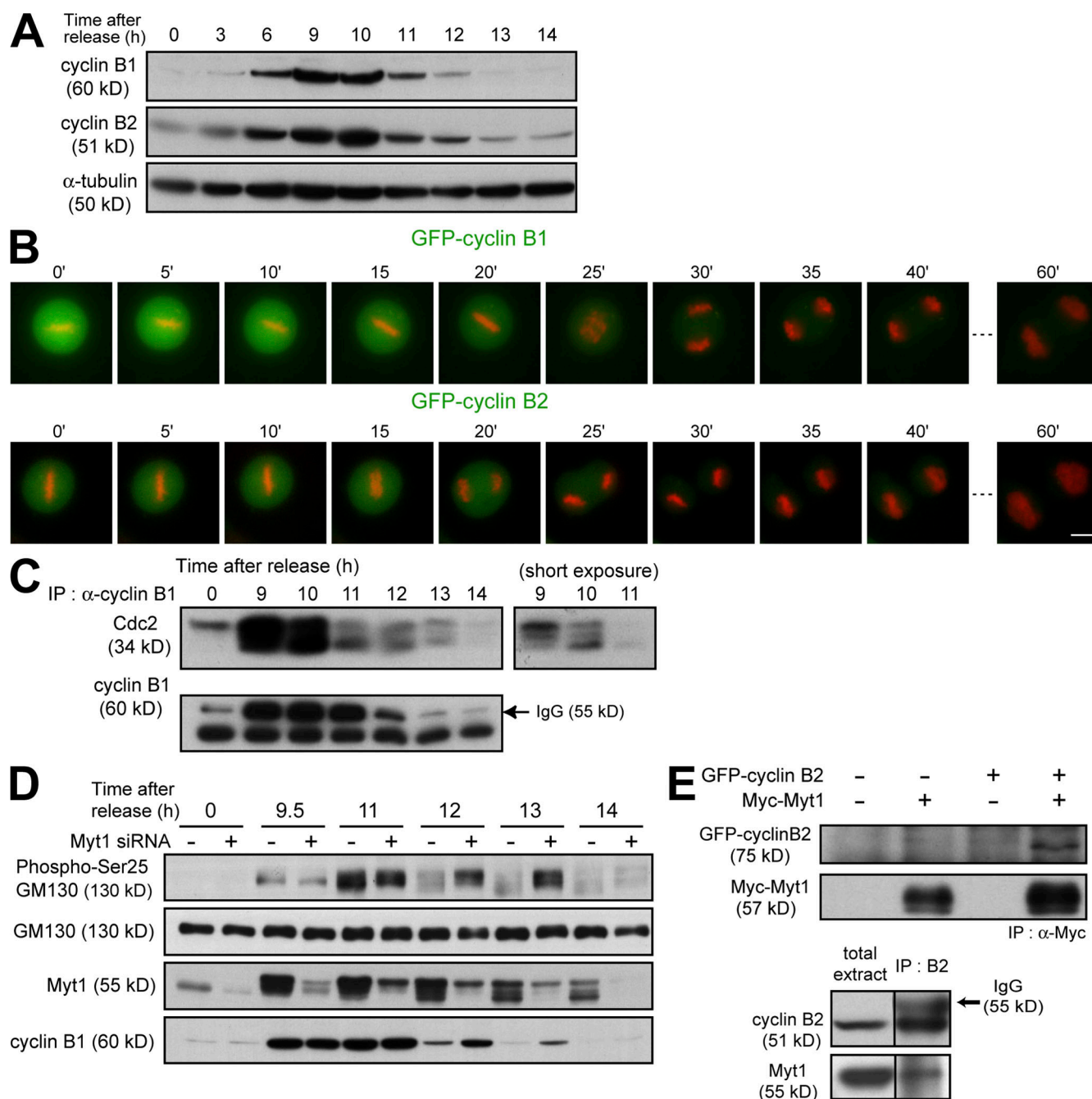
Figure 8. **Residual cyclin B–Cdc2 during mitotic exit.** (A) Extracts from HeLa cells synchronized by a double-thymidine block were analyzed by SDS-PAGE followed by immunoblotting with anti–cyclin B1, anti–cyclin B2, and anti–α-tubulin antibodies. (B) HeLa cells were transfected with GFP–cyclin B1 or GFP–cyclin B2 together with DsRed–histone H1 and were monitored by time-lapse video microscopy. Time-lapse sequences taken every 5 min from metaphase to mitotic exit are shown. These data are representative of >10 cells in separate experiments. Time is given in minutes. (C) Extracts from HeLa cells synchronized by a double-thymidine block were analyzed by immunoprecipitation with antibody against cyclin B1 followed by immunoblotting with antibodies against Cdc2 and cyclin B1. The image with short exposure time on the same gel is shown in the right panel. (D) HeLa cells were transfected with or without Myt1 siRNA in the interval between the two thymidine blocks. The cell extracts were subjected to immunoblotting with antiphospho-Ser25-GM130, anti-GM130, anti-Myt1, and anti–cyclin B1 antibodies. (E) Myc-tagged Myt1 was coexpressed with GFP–cyclin B2, and the cells were analyzed by immunoprecipitation with antibody against Myc followed by immunoblotting with antibodies against GFP and Myc (top). HeLa cells that were synchronized by a double-thymidine block were treated with 125 ng/ml nocodazole 8.5 h after the release and were harvested up to 12 h to gather mitotically arrested cells. The cells were analyzed by immunoprecipitation with antibody against cyclin B2 followed by immunoblotting with antibodies against cyclin B2 and Myt1 (bottom). Bar, 10 μm.

remained in late M phase and even early G1 phase (Fig. 8 A). To examine the levels of cyclin B1 and cyclin B2 in more detail, we performed time-lapse video microscopy experiments. Synchronized HeLa cells were transfected with GFP–cyclin B1 or

–cyclin B2 together with DsRed–histone H1 and were monitored during mitosis by time-lapse video microscopy. We confirmed that the protein levels of GFP–cyclin B1 and GFP–cyclin B2 were comparable with, or, at most, were less than three times the
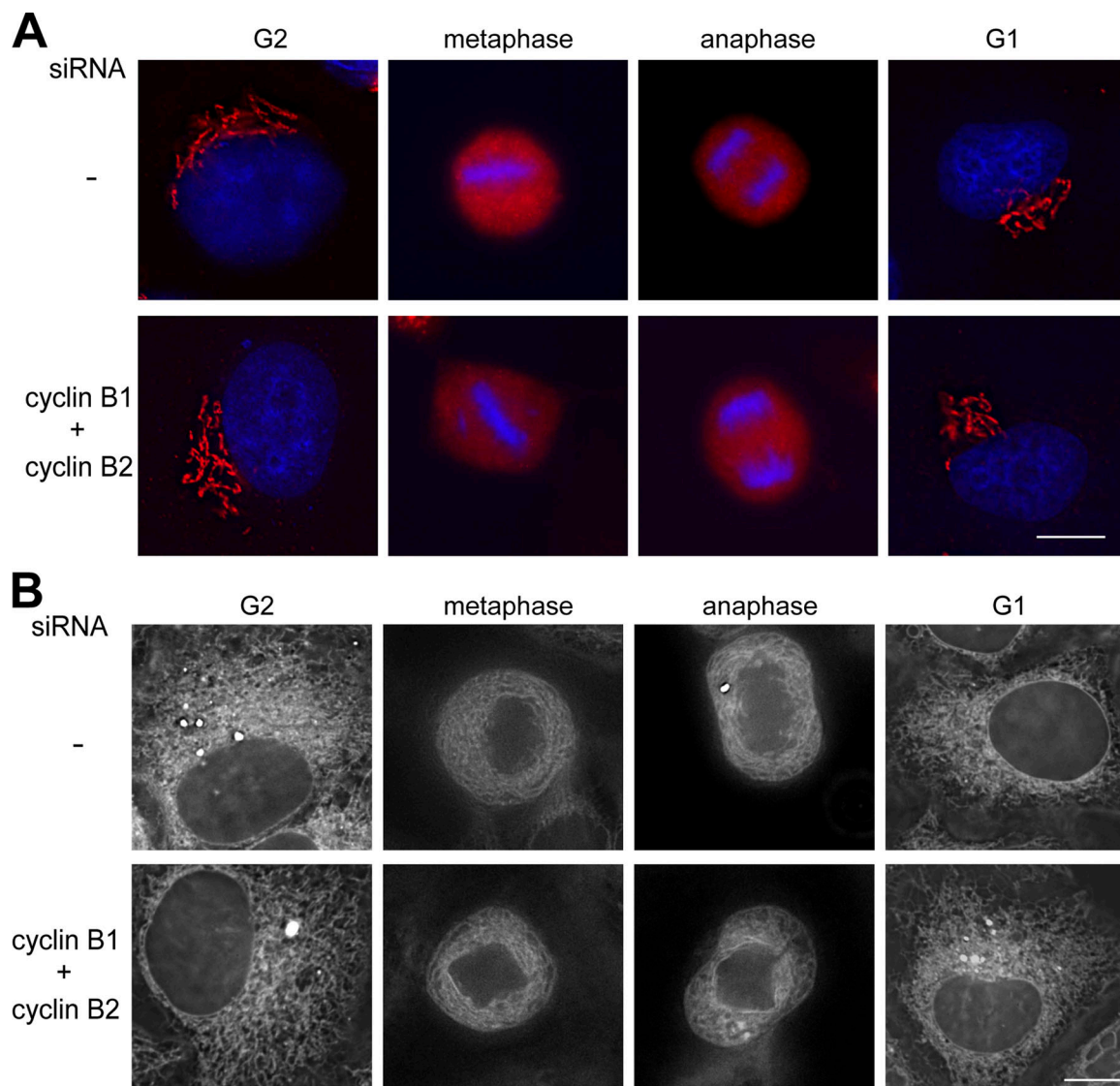
Figure 9. **Golgi fragmentation/reassembly and morphological changes of ER occur almost normally during mitosis in cyclin B1/cyclin B2 double siRNA–treated cells.** HeLa cells were transfected with cyclin B1 and cyclin B2 siRNAs in the interval between the two thymidine blocks. (A) The cells at 8 (G2), 11 (metaphase and anaphase), and 18 h (G1) after the release were stained with anti-GM130 antibody (red) and Hoechst (blue). (B) ER was visualized with ER tracker red in living cells at 8 (G2), 11–12 (metaphase and anaphase), and 18 h (G1) after the release. Bars, 10 μm.

levels of endogenous cyclin B1 and cyclin B2, respectively (unpublished data). Although GFP–cyclin B1 began to be degraded at metaphase as previously reported (Clute and Pines, 1999), GFP–cyclin B2 began to be degraded after metaphase (Fig. 8 B). Most importantly, low but significant levels of both GFP–cyclin B1 and GFP–cyclin B2 persisted even in anaphase and telophase (Fig. 8 B). These data suggest that when Golgi and ER reassembly occur during telophase, low levels of B-type cyclins are present as partners of Cdc2. As Cdc2 activity plays a role in promoting Golgi disassembly and ER network reorganization to the M-phase type during early mitosis, it is likely that the kinase activity of Cdc2 must be suppressed during telophase; otherwise, the kinase activity would prevent Golgi and ER reassembly. We hypothesized that Myt1 inhibits Cdc2 activity during telophase.

If our hypothesis is correct, Cdc2 would be phosphorylated on Thr14/Tyr15 during mitotic exit. To address this, we examined the phosphorylation state of Cdc2 in the cyclin B1–Cdc2 complex

in synchronized HeLa cells by immunoblotting. The decreased gel mobility of Cdc2 is known to be caused by the phosphorylation of Thr14 and Tyr15 (Norbury et al., 1991; Solomon et al., 1992). The obtained results have clearly demonstrated that Cdc2, which was coprecipitated with cyclin B1, was mostly phosphorylated on both Thr14 and Tyr15 in late G2 at 9 h, and the major population of Cdc2 was the dephosphorylated form at the onset of mitosis at 10 h (Fig. 8 C). Most importantly, just before cyclin B1 disappeared in late mitosis, the amount of phosphorylated Cdc2 became similar to or greater than that of unphosphorylated Cdc2 (at 13 h; Fig. 8 C). In seven independent experiments, we obtained similar results. Consistent with our results, Jin et al. (1998) previously showed that when a stabilized form of cyclin B1 was expressed in synchronized HeLa cells, Cdc2 phosphorylation was increased during mitotic exit, and the cells were capable of exiting mitosis. Thus, our results and the results of Jin et al. (1998) strongly suggest that there is

an increase in phospho-Thr14/Tyr15 of Cdc2 during mitotic exit. Furthermore, we have revealed that the phosphorylation of GM130 on Ser25, which is one of the targets of Cdc2 on the Golgi (Lowe et al., 1998, 2000), persisted for a prolonged period during mitotic exit in synchronized Myt1-depleted HeLa cells compared with control cells (Fig. 8 D). This result suggests that residual cyclin B–Cdc2 should be suppressed by Myt1 during mitotic exit.

It has previously been shown that Myt1 associates with cyclin B1 (Liu et al., 1999). Thus, we tested whether Myt1 associates with cyclin B2 as well. When Myc-tagged Myt1 was coexpressed with GFP–cyclin B2, Myc-Myt1 coprecipitated with GFP–cyclin B2 (Fig. 8 E, top). Moreover, Myc-Myt1 colocalized with GFP–cyclin B2 (unpublished data). In addition, endogenous Myt1 coprecipitated with endogenous cyclin B2 in mitotic HeLa cells (Fig. 8 E, bottom). These results suggest that both cyclin B1–Cdc2 and cyclin B2–Cdc2 could be targets of Myt1 and that both activities might be suppressed by Myt1 during Golgi and ER reassembly at the end of mitosis. To test this, we inhibited cyclin B1 and cyclin B2 expression by siRNA in Myt1 siRNA-treated and untreated asynchronous HeLa cells (see Fig. 10 A). Although the single siRNA treatment for each target almost completely depleted the cells of the target, it was difficult to find the conditions in which the triple siRNA treatment for cyclin B1, cyclin B2, and Myt1 could almost completely abolish the expression of three proteins. Thus, under the conditions we used here, cyclin B1 expression was almost completely inhibited, but low levels of Myt1 and cyclin B2 expression remained (see Fig. 10 A). However, this level of Myt1 down-regulation (∼90% depletion) induced the Golgi and ER morphology defects (see Fig. 10, B and C), which were indistinguishable from those resulting from the almost complete loss of Myt1, as shown in Figs. 3 A and 5 A. Cyclin B1 and/or cyclin B2 down-regulation in combination or alone in Myt1 siRNA-untreated cells had little effect on the Golgi and ER morphology both in interphase and in M phase; that is, even in cyclin B1/cyclin B2 double siRNA–treated synchronized HeLa cells, the Golgi fragmentation and reassembly during mitosis occurred almost normally (Fig. 9 A), and ER meshwork changes during mitosis also occurred almost normally (Fig. 9 B), although a significant proportion (∼30%) of cyclin B1/cyclin B2 double siRNA–treated cells displayed micronuclei or multinuclei (Fig. 10 B and not depicted). Either cyclin B1 or cyclin B2 down-regulation in Myt1 siRNA-treated cells partially rescued the Golgi and ER morphology defects seen in Myt1-depleted cells. Remarkably, both cyclin B1 and cyclin B2 down-regulation almost completely rescued the defects (Fig. 10, B–D); in the Myt1/cyclin B1/cyclin B2 triple siRNA–treated cells, the Golgi apparatus resumed a normal ribbonlike appearance (Fig. 10 B), and ER resumed a fine interphase-type meshwork (Fig. 10, C and D). The significant proportion of Myt1/cyclin B1/B2 triple siRNA–treated cells also displayed micronuclei or multinuclei. Even in these cells, the normal ribbonlike appearance of the Golgi apparatus and fine ER meshwork was almost completely restored (Fig. 10, B–D). These results strongly suggest that Myt1 facilitates Golgi and ER reassembly by suppressing both cyclin B1– and cyclin B2–Cdc2 activities.

Discussion

In this study, we have examined the role of Myt1 in mammalian somatic cell cycles. We first show that inhibition of Myt1 expression by siRNA in HeLa cells does not change the timing of mitotic entry but rather induces severe defects in the morphology of the Golgi and ER, resulting in abnormally condensed Golgi structures and disrupted ER meshwork. Our results then show that the Golgi and ER morphology defects are observed after the cells pass through mitosis. These results demonstrate that Myt1 is required for Golgi and ER reassembly during mitotic exit, not for the biogenesis or maintenance of Golgi and ER structures during interphase. Moreover, our finding that add back of wild-type but not kinase-inactive Myt1 rescues the Golgi and ER reassembly defects seen in Myt1-depleted cells demonstrates that the kinase activity of Myt1 is required for Golgi and ER reassembly. Myt1 is known to bind to cyclin B1, and here it is shown to bind to cyclin B2 as well. Remarkably, inhibition of both cyclin B1 and cyclin B2 expression by siRNAs markedly rescues the Myt1 siRNA-induced Golgi and ER reassembly defects. These results strongly suggest that Myt1 functions to facilitate Golgi and ER reassembly during mitotic exit by suppressing both cyclin B1– and cyclin B2–Cdc2 activities. We have also found that Wee1 siRNA-treated HeLa cells enter mitosis much earlier than the control and Myt1 siRNA-treated cells. However, it has previously been reported that expression of Cdc2AF (a mutant form of Cdc2 in which Thr14 and Tyr15 are changed to Ala and Phe) in HeLa cells to levels that markedly elevate histone H1 activity does not advance the timing of nuclear envelope breakdown or chromatin condensation (Blasina et al., 1997; Jin et al., 1998). This result indicates that the activation of Cdc2 is not sufficient to induce nuclear envelope breakdown or chromatin condensation. Therefore, we may speculate that Wee1 has an additional role. For example, Wee1 might inhibit the nuclear accumulation of cyclin B1–Cdc2, or Wee1 might inhibit cyclin B–Cdc2 by its direct interaction. Future studies are needed to analyze the phenotypes of Wee1 knockdown cells in more detail.

Mitotic Golgi fragmentation and reassembly are crucial events in mammalian cells. Golgi fragmentation is thought to facilitate the equal partitioning of Golgi membranes between the two daughter cells during cell division (Shorter and Warren, 2002) and has recently been reported to be important for mitotic progression (Sutterlin et al., 2002; Hidalgo Carcedo et al., 2004). Golgi reassembly, then, is an essential process for establishing a functional Golgi apparatus (Shorter and Warren, 2002). Mitotic Golgi fragmentation in mammalian cells is dependent on Cdc2 (Lowe et al., 1998). Golgi proteins such as GM130, GRASP65, p47, and Rab1, which play a crucial role in heterotypic or homotypic membrane fusion or stacking of Golgi cisternae, are substrates of Cdc2 (Shorter and Warren, 2002). Cdc2-mediated phosphorylation of these Golgi proteins is expected to promote mitotic Golgi disassembly through the cessation of vesicle transport and unstacking of existing cisternae. Thus, during telophase, these phosphoproteins must be dephosphorylated for proper Golgi reassembly to occur. Therefore, the active Cdc2 would need to be inactivated during telophase to ensure Golgi reassembly. Our results with cyclin B1 and cyclin B
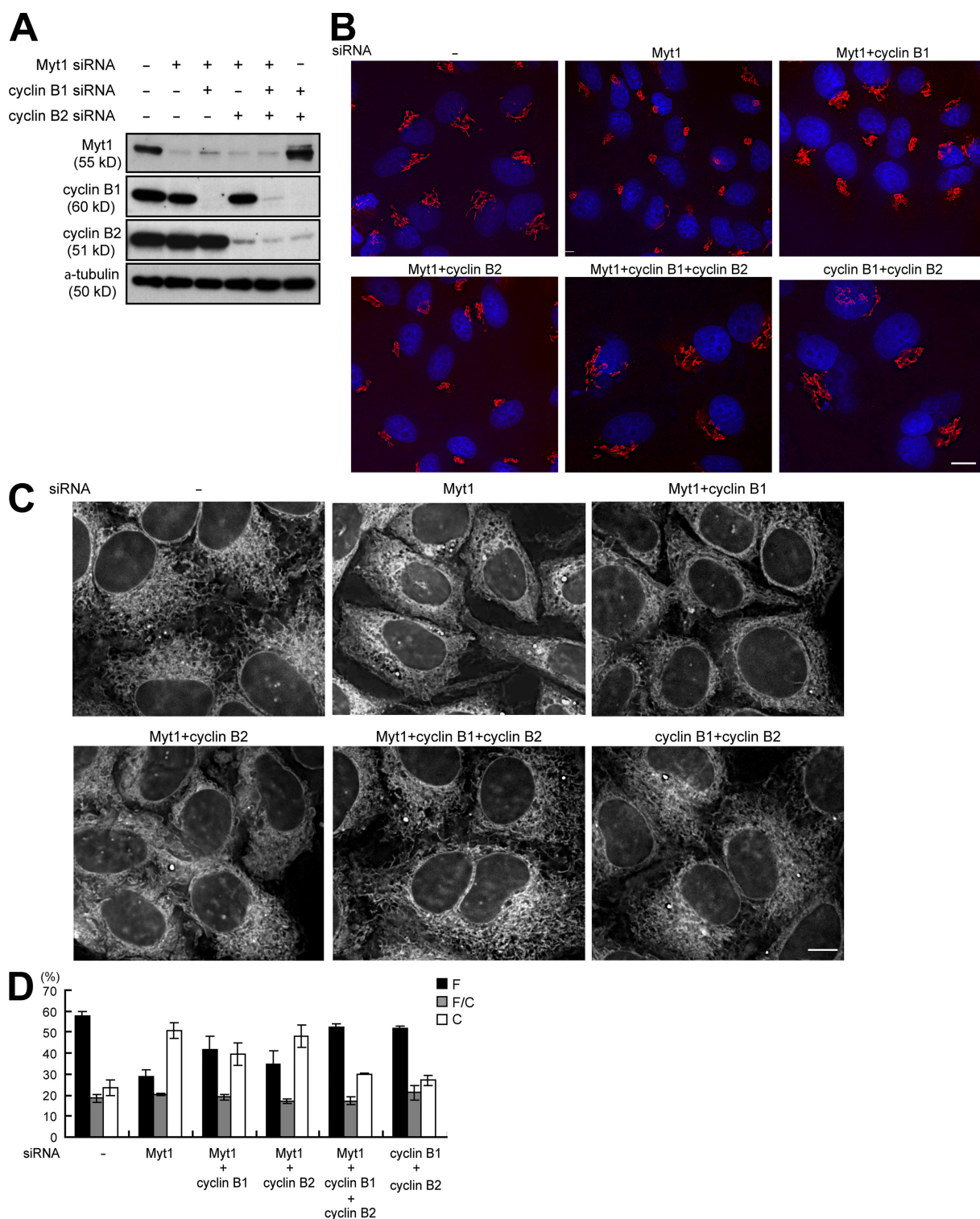
Figure 10. **Myt1 functions to facilitate Golgi and ER assembly through both cyclin B1 and cyclin B2.** HeLa cells were transfected with Myt1, cyclin B1, or cyclin B2 siRNA (alone or in combination) and incubated for 48 h. (A) The cells were subjected to immunoblotting with antibodies against Myt1, cyclin B1, cyclin B2, and α-tubulin. (B) The cells were fixed and stained with anti-GM130 antibody (red) and Hoechst (blue). (C) ER was visualized with ER tracker red in living HeLa cells. (D) The cells in C were classified into three types based on the ER morphology as described in Fig. 5 B. More than 45 cells were examined in each experiment, and experiments were performed more than twice. The cells were subjected to immunoblotting with antibodies against Myt1, cyclin B1, cyclin B2, and α-tubulin. Error bars represent ±SD. F, fine meshwork type; C, coarse meshwork type; F/C, fine/coarse meshwork type. Bars, 10 μm.

B2 down-regulation experiments strongly suggest that Myt1 facilitates Golgi reassembly through inhibition of both cyclin B1– and cyclin B2–Cdc2 activities during telophase.

ER is a continuous membrane system enclosing a single luminal space and comprises tubular networks and cisternae throughout the cytoplasm (Voeltz et al., 2002; Shibata et al., 2006).

Even during mitosis, the continuity of the luminal side of the organelle is maintained (Ellenberg et al., 1997; Terasaki, 2000). However, the precise structural features of the ER network in mitotic cells are less clear. The round shape of mitotic cells makes it difficult to observe the precise structures of the ER. In this study, we show that Myt1 is essential for ER meshwork formation during mitotic exit but not for its maintenance in interphase. This result suggests that ER may undergo dynamic morphological changes during mitosis. Furthermore, our data show that Myt1 facilitates reassembly of a fine interphase-type ER meshwork during mitotic exit through inhibition of cyclin B1 and cyclin B2. This finding suggests that Cdc2 activity may play a pivotal role in dynamic morphological changes of ER during mitosis. Previous studies also suggested that Cdc2 might be involved in the regulation of ER morphology (Dreier and Rapoport, 2000; Kano et al., 2005). In semi-intact cells, an elaborate meshwork of ER is disrupted by a mitotic cytosol, and the disruption is dependent on Cdc2 kinase (Kano et al., 2005). In vitro, de novo formation of ER meshwork from microsomal vesicles occurs in interphase extracts but not in Cdc2 kinase–activated interphase extracts (Dreier and Rapoport, 2000). Thus, Cdc2 activity has the ability to disrupt the elaborate ER meshwork. These results are in agreement with our idea that Myt1-mediated inhibition of Cdc2 activity during mitotic exit is important for the formation of an elaborate ER meshwork.

Cdc2 activities associated with B-type cyclins have been thought to play an important role in inducing a broad range of mitotic events, including mitotic Golgi fragmentation. However, our results show that even when both cyclin B1 and cyclin B2 expression are inhibited, the Golgi fragmentation and reassembly during mitosis occur almost normally, and ER meshwork changes during mitosis also occur almost normally (Fig. 9). These observations suggest that cyclin B1 and cyclin B2 are dispensable for Golgi fragmentation and ER reorganization during early mitosis. Most recently, Gong et al. (2007) reported that the timing of nuclear envelope breakdown was affected very little by knocking down both cyclin B1 and cyclin B2 but was markedly delayed by knocking down cyclin A2. Gong et al. (2007) then also concluded that cyclin A2 is crucial for nuclear envelope breakdown. Thus, it is likely that cyclin A2, both in the absence or presence of cyclin B1 and cyclin B2, may play a pivotal role in Golgi disassembly and ER network reorganization during mitosis, although it is also possible that very low levels of cyclin B1 and cyclin B2, which remain in cyclin B1/cyclin B2 double siRNA–treated cells, play a role in these processes in combination with cyclin A2. Cyclin A2, which is thus implicated in the early mitotic events, is always degraded before cyclin B1 and cyclin B2 (den Elzen and Pines, 2001). Although cyclin B1 and cyclin B2 are mostly degraded at metaphase/anaphase, both cyclin B1 and cyclin B2 proteins appear to be present at very low levels during late mitosis (Fig. 10 A). Thus, when Golgi and ER reassembly occur during telophase, the low levels of B-type cyclins are present as partners of Cdc2. Because the kinase activity of the remaining cyclin B1– and cyclin B2–Cdc2 would prevent Golgi and ER reassembly, their activities must be suppressed during mitotic exit. Our results suggest that Myt1 might inhibit both cyclin B1– and cyclin

B2–Cdc2 activities during mitotic exit for proper Golgi and ER reassembly to occur, although we cannot exclude the possibility that Myt1 has other unidentified targets.

Our results also suggest that Myt1-mediated suppression of cyclin B1– and cyclin B2–Cdc2 activities may not be indispensable for the regulation of a broad range of mitotic events, such as regulation of mitotic entry timing and spindle assembly, although we cannot exclude the possibility that the depletion of Myt1 was insufficient to yield the phenotype. However, it is certain that the effect of Myt1 depletion was primarily seen in Golgi and ER reassembly, not in mitotic entry timing. How can such a difference of the effects of Myt1 depletion arise? It does not seem to depend on the cyclin-type specificity of Myt1 because Myt1 inhibits not only cyclin B1–Cdc2 activity but also cyclin A2–Cdc2 activity in vitro (Booher et al., 1997). We speculate that the inhibitory effect of Myt1 toward Cdc2 may not be strong enough to inhibit the whole population of cyclin–Cdc2 complexes at G2/M phase, in which total A- and B-type cyclins are abundant. In contrast, because the protein levels of Cdc2–cyclins are very low in late mitosis, Myt1 may inhibit Cdc2 activity completely, and the effect of Myt1 may become prominent in this period. Thus, we think that the difference of the effects of Myt1 on mitotic entry timing and Golgi/ER reassembly may arise from the limited inhibitory effect of Myt1 toward Cdc2. In summary, we have revealed that Myt1 is required for the control of intracellular membrane dynamics such as Golgi and ER reassembly during mitosis in mammalian somatic cell cycles.

Materials and methods

Cell culture and synchronization

HeLa cells were cultured in DME containing 10% FBS or 10% calf serum. To synchronize cells, HeLa cells were arrested at the G1/S boundary by a double-thymidine block and were released from the arrest by washing with fresh medium. 50 μM MG132 (EMD) was added into the medium 8 h after the release from double-thymidine block and was incubated. For transfection with DNA vectors and siRNAs during synchronization, cells were transfected with DNA vectors in Opti-MEM with the use of Lipofectamine Plus (Invitrogen) for 1 h and were washed into fresh medium containing thymidine for the first block. Then, cells were transfected with siRNAs by the use of Oligofectamine (Invitrogen) after the first thymidine block. For time-lapse imaging, synchronized HeLa cells were transfected with DNA vectors in Opti-MEM with the use of Lipofectamine Plus for 1 h and were washed into fresh medium containing thymidine for the second block.

Immunoblotting

Cells were lysed in lysis buffer (50 mM Tris, pH 8.0, 100 mM NaCl, 5 mM EDTA, 0.5% NP-40, 2 mM DTT, 1 mM PMSF, 1 mM Na$_3$VO$_4$, and 2 μg/ml aprotinin) and centrifuged at 20,000 g for 15 min. The cell extracts were subjected to immunoblotting with anti-Myt1 (Liu et al., 1997), anti–cyclin B1 (Santa Cruz Biotechnology, Inc.), anti–α-tubulin (Sigma-Aldrich), anti-Wee1 (Santa Cruz Biotechnology, Inc.), anti–cyclin B2 (Santa Cruz Biotechnology, Inc.), anti-Cdc2 (Santa Cruz Biotechnology, Inc.), anti–c-Myc (Santa Cruz Biotechnology, Inc.), antiphospho-Ser25-GM130 (provided by M. Lowe, University of Manchester, Manchester, UK; Lowe et al., 2000), anti-GM130 (BD Biosciences), or anti-GFP antibody (Living Colors; BD Biosciences).

Phosphatase treatment

Cells were lysed in phosphatase buffer (50 mM Hepes, pH 7.5, 100 mM NaCl, 0.1 mM EGTA, 0.5% NP-40, 2 mM DTT, 1 mM PMSF, 2 mM MnCl$_2$, and 2 μg/ml aprotinin) and centrifuged at 20,000 g for 15 min. The cell extracts were incubated with 300 U of purified λ protein phosphatase (New England Biolabs, Inc.) for 45 min at 30°C. The phosphatase reaction was stopped by the addition of the SDS sample buffer. Samples were analyzed by immunoblotting.

Cell staining and microscopy

Cells were fixed for 10 min with 3.7% formaldehyde and permeabilized for 10 min with 0.5% Triton X-100 in PBS. Cells were blocked for 1 h with 3% BSA, incubated overnight with primary antibodies (anti-GM130 and anti-p115 antibodies were purchased from BD Biosciences; anti-LAMP1 antibody was purchased from Santa Cruz Biotechnology, Inc.; antiphosphohistone H3 antibody was obtained from Millipore; anti–γ-adaptin and anti–γ-tubulin antibodies were purchased from Sigma-Aldrich; and anti-Myt1 [Liu et al., 1997] and anti-Sec13 [Kano et al., 2004] antibodies were described previously), washed, and incubated for 1 h with secondary antibodies (AlexaFluor488 or 594 goat anti–mouse or anti–rabbit IgG antibodies; Invitrogen). To stain the actin cytoskeleton, AlexaFluor546 phalloidin was used. For ER tracker (Invitrogen) labeling, cells were incubated with 1 μM ER tracker red for 30 min before imaging without fixation. Images of Fig. 3 A (left) and Fig. 4 A were acquired using a microscope (Axiophot2; Carl Zeiss, Inc.), a 63× 1.4 NA oil objective lens (Carl Zeiss, Inc.), a CCD camera (Quantix 1400-G2; Photometrics), and IPLab Spectrum software (BD Biosciences). All other images were acquired using the DeltaVision system (Applied Precision) equipped with an inverted microscope (IX71; Olympus), a 60× 1.4 NA oil objective lens (Olympus), a CCD camera (CoolSNAP HQ Monochrome; Photometrics), and SoftWoRx software (Applied Precision). In the images of Figs. 2, 3 (A [right] and C), 5 (A and C), 7 (A), 9, and 10 (B and C), deconvolving images were performed by using SoftWoRx. Image analysis was performed using either SoftWoRx or Photoshop (Adobe). Time-lapse images were acquired by using a DeltaVision Image Restoration microscope with SoftWoRx software with a temperature-controlled stage. During acquisition, cells were cultured at 37°C in the medium with 20 mM Hepes, pH 7.3, in glass-bottom chambers. The cells at prophase and prometaphase were subjected to the time-lapse imaging. Time-lapse images were taken every 5 min.

siRNA and add-back experiment

RNA oligonucleotides (21 nucleotides) homologous to human Myt1, cyclin B1, and cyclin B2 were designed as follows: Myt1 forward (5′-GUGACAU-CAACUCAGAGCCTT-3′) and Myt1 reverse (5′-GGCUCUCGAGUUGAU-GUCACTT-3′); cyclin B1 forward (5′-UGAAGAUUCUAAGAGCUUUTT-3′) and cyclin B1 reverse (5′-AAAGCUCUUAGAAUCUUCATT-3′); and cyclin B2 forward (5′-GAGAAUCUCUGCCAAGCUUTT-3′) and cyclin B2 reverse (5′-AAGCUUGGCAGAGAUUCUCTT-3′). Cells were transfected with annealed siRNAs by the use of Oligofectamine (Invitrogen). In Figs. 1–8, cells grown in a six-well dish were transfected with 200 pmol Myt1 or Wee1 siRNA. In these conditions, single siRNA treatment for each target almost completely depleted the cells of the target (Figs. 1 B and 6 A). However, it was difficult to find the conditions in which the triple siRNA treatment for Myt1, cyclin B1, and cyclin B2 could almost completely abolish the expression of three proteins. In Fig. 10, cells were transfected with 400 pmol Myt1 siRNA, 100 pmol cyclin B1 siRNA, and 20 pmol cyclin B2 siRNA for the triple siRNA treatment. In this condition, cyclin B1 expression was almost completely inhibited, but low levels of Myt1 and cyclin B2 expression remained (Fig. 10 A). We found that when cells were transfected with 100 pmol of single Myt1 siRNA, the remaining Myt1 protein levels were the same as the remaining Myt1 levels in Myt1/cyclin B1/cyclin B2 triple siRNA–treated cells (Fig. 10 A), and this level of Myt1 down-regulation (∼90% depletion) induced the Golgi and ER morphology defects (Fig. 10, B and C), which were indistinguishable from those resulting from the almost complete loss of Myt1. In Fig. 10, cells were transfected with 200 pmol Myt1 siRNA and 100 pmol cyclin B1 siRNA for the double siRNA treatment for Myt1 and cyclin B1 and were transfected with 400 pmol Myt1 siRNA and 20 pmol cyclin B2 siRNA for the double siRNA treatment for Myt1 and cyclin B2. Also, in Figs. 9 and 10, cells were transfected with 100 pmol cyclin B1 siRNA and 20 pmol cyclin B2 siRNA for the double siRNA treatment for cyclin B1 and cyclin B2. In all siRNA experiments in this manuscript, control means the procedure without siRNA. We also confirmed that there was no change in the Golgi and ER morphology when we used Luciferase siRNA as control siRNA. Silent mutations in the siRNA-targeting region of Myt1 were introduced by PCR-based mutagenesis using the following primers: forward (5′-GACATCAACTC**T**GA**A**CCTCCTCGGGGCTC-3′; bold nucleotides indicate silent mutations) and reverse (5′-GAGCCCCGAG-GAGGTTCAGAGTTGATGTC-3′). For add-back experiments, the cells were transfected with 0.02 μg pCDNA3 vector harboring the siRNA-resistant form of Myt1 together with 0.5 μg pECFP vector in Opti-MEM with the use of Lipofectamine Plus for 1 h before the first thymidine block.

Immunoprecipitation

Transient transfection with GFP–cyclin B2 and Myc-Myt1 was performed using FuGENE6 (Roche) according to the manufacturer's instructions. For immunoprecipitation experiments, cells were lysed in lysis buffer and homogenized.

Cell lysates were incubated for 2 h at 4°C with anti–cyclin B1, anti–c-Myc, or anti–cyclin B2 antibody (Santa Cruz Biotechnology, Inc.), and protein A–Sepharose beads (GE Healthcare) were added and incubated for 2 h. The precipitates were then washed three times with lysis buffer. The proteins were separated by SDS-PAGE and analyzed by immunoblotting.

Electron microscopy

Transmission electron microscopic observations were conducted as described previously (Yonemura et al., 1995). For immunolabeling, HeLa cells were fixed for 10 min with 4% PFA and permeabilized for 10 min with 0.002% saponin in PBS. Cells were blocked for 1 h with 3% BSA, incubated overnight with anti-GM130 antibody, and washed. After incubation with 1.4-nm colloidal gold-conjugated secondary antibodies (Nanoprobe), samples were fixed with 1% glutaraldehyde in 0.1 M phosphate buffer, pH 7.4, for 10 min, and the gold particles were intensified by use of an HQ silver kit (Nanoprobe). The samples were postfixed in 0.1% osmium tetroxide for 90 min on ice, stained with 0.5% uranyl acetate for 2 h, dehydrated through graded concentrations of ethanol, and embedded in epoxy resin.

Golgi area

Anti-GM130 antibody staining images were obtained using a DeltaVision Image Restoration microscope with SoftWoRx software. All images were taken in the same exposure time. Using Photoshop, the acquired images were binarized to white and black using the fixed threshold in all samples in each experiment. The white area represents the Golgi apparatus, and white pixels were measured as relative Golgi area.

References

Blasina, A., E.S. Paegle, and C.H. McGowan. 1997. The role of inhibitory phosphorylation of CDC2 following DNA replication block and radiation-induced damage in human cells. *Mol. Biol. Cell.* 8:1013–1023.

Booher, R.N., P.S. Holman, and A. Fattaey. 1997. Human Myt1 is a cell cycle-regulated kinase that inhibits Cdc2 but not Cdk2 activity. *J. Biol. Chem.* 272:22300–22306.

Burrows, A.E., B.K. Sceurman, M.E. Kosinski, C.T. Richie, P.L. Sadler, J.M. Schumacher, and A. Golden. 2006. The *C. elegans* Myt1 ortholog is required for the proper timing of oocyte maturation. *Development.* 133:697–709.

Clute, P., and J. Pines. 1999. Temporal and spatial control of cyclin B1 destruction in metaphase. *Nat. Cell Biol.* 1:82–87.

den Elzen, N., and J. Pines. 2001. Cyclin A is destroyed in prometaphase and can delay chromosome alignment and anaphase. *J. Cell Biol.* 153:121–136.

Dreier, L., and T.A. Rapoport. 2000. In vitro formation of the endoplasmic reticulum occurs independently of microtubules by a controlled fusion reaction. *J. Cell Biol.* 148:883–898.

Ellenberg, J., E.D. Siggia, J.E. Moreira, C.L. Smith, J.F. Presley, H.J. Worman, and J. Lippincott-Schwartz. 1997. Nuclear membrane dynamics and reassembly in living cells: targeting of an inner nuclear membrane protein in interphase and mitosis. *J. Cell Biol.* 138:1193–1206.

Gong, D., J.R. Pomerening, J.W. Myers, C. Gustavsson, J.T. Jones, A.T. Hahn, T. Meyer, and J.E. Ferrell Jr. 2007. Cyclin A2 regulates nuclear-envelope breakdown and the nuclear accumulation of cyclin B1. *Curr. Biol.* 17:85–91.

Heald, R., M. McLoughlin, and F. McKeon. 1993. Human wee1 maintains mitotic timing by protecting the nucleus from cytoplasmically activated Cdc2 kinase. *Cell.* 74:463–474.

Hidalgo Carcedo, C., M. Bonazzi, S. Spano, G. Turacchio, A. Colanzi, A. Luini, and D. Corda. 2004. Mitotic Golgi partitioning is driven by the membrane-fissioning protein CtBP3/BARS. *Science.* 305:93–96.

Hunt, T. 1991. Cyclins and their partners: from a simple idea to complicated reality. *Semin. Cell Biol.* 2:213–222.

Jin, P., S. Hardy, and D.O. Morgan. 1998. Nuclear localization of cyclin B1 controls mitotic entry after DNA damage. *J. Cell Biol.* 141:875–885.

Jin, Z., E.M. Homola, P. Goldbach, Y. Choi, J.A. Brill, and S.D. Campbell. 2005. *Drosophila* Myt1 is a Cdk1 inhibitory kinase that regulates multiple aspects of cell cycle behavior during gametogenesis. *Development.* 132:4075–4085.

Kano, F., A.R. Tanaka, S. Yamauchi, H. Kondo, and M. Murata. 2004. Cdc2 kinase-dependent disassembly of endoplasmic reticulum (ER) exit sites inhibits ER-to-Golgi vesicular transport during mitosis. *Mol. Biol. Cell.* 15:4289–4298.

Kano, F., H. Kondo, A. Yamamoto, A.R. Tanaka, N. Hosokawa, K. Nagata, and M. Murata. 2005. The maintenance of the endoplasmic reticulum network is regulated by p47, a cofactor of p97, through phosphorylation by cdc2 kinase. *Genes Cells.* 10:333–344.

Kornbluth, S., B. Sebastian, T. Hunter, and J. Newport. 1994. Membrane localization of the kinase which phosphorylates p34cdc2 on threonine 14. *Mol. Biol. Cell.* 5:273–282.

Lamitina, S.T., and S.W. L'Hernault. 2002. Dominant mutations in the *Caenorhabditis elegans* Myt1 ortholog wee-1.3 reveal a novel domain that controls M-phase entry during spermatogenesis. *Development.* 129:5009–5018.

Lew, D.J., and S. Kornbluth. 1996. Regulatory roles of cyclin dependent kinase phosphorylation in cell cycle control. *Curr. Opin. Cell Biol.* 8:795–804.

Lippincott-Schwartz, J., T.H. Roberts, and K. Hirschberg. 2000. Secretory protein trafficking and organelle dynamics in living cells. *Annu. Rev. Cell Dev. Biol.* 16:557–589.

Liu, F., J.J. Stanton, Z. Wu, and H. Piwnica-Worms. 1997. The human Myt1 kinase preferentially phosphorylates Cdc2 on threonine 14 and localizes to the endoplasmic reticulum and Golgi complex. *Mol. Cell. Biol.* 17:571–583.

Liu, F., C. Rothblum-Oviatt, C.E. Ryan, and H. Piwnica-Worms. 1999. Overproduction of human Myt1 kinase induces a G2 cell cycle delay by interfering with the intracellular trafficking of Cdc2-cyclin B1 complexes. *Mol. Cell. Biol.* 19:5113–5123.

Lowe, M., C. Rabouille, N. Nakamura, R. Watson, M. Jackman, E. Jamsa, D. Rahman, D.J. Pappin, and G. Warren. 1998. Cdc2 kinase directly phosphorylates the cis-Golgi matrix protein GM130 and is required for Golgi fragmentation in mitosis. *Cell.* 94:783–793.

Lowe, M., N.K. Gonatas, and G. Warren. 2000. The mitotic phosphorylation cycle of the cis-Golgi matrix protein GM130. *J. Cell Biol.* 149:341–356.

McGowan, C.H., and P. Russell. 1993. Human Wee1 kinase inhibits cell division by phosphorylating p34cdc2 exclusively on Tyr15. *EMBO J.* 12:75–85.

Mueller, P.R., T.R. Coleman, A. Kumagai, and W.G. Dunphy. 1995. Myt1: a membrane-associated inhibitory kinase that phosphorylates Cdc2 on both threonine-14 and tyrosine-15. *Science.* 270:86–90.

Nakajo, N., S. Yoshitome, J. Iwashita, M. Iida, K. Uto, S. Ueno, K. Okamoto, and N. Sagata. 2000. Absence of Wee1 ensures the meiotic cell cycle in *Xenopus* oocytes. *Genes Dev.* 14:328–338.

Nguyen, T.B., K. Manova, P. Capodieci, C. Lindon, S. Bottega, X.Y. Wang, J. Refik-Rogers, J. Pines, D.J. Wolgemuth, and A. Koff. 2002. Characterization and expression of mammalian cyclin b3, a prepachytene meiotic cyclin. *J. Biol. Chem.* 277:41960–41969.

Nigg, E.A. 2001. Mitotic kinases as regulators of cell division and its checkpoints. *Nat. Rev. Mol. Cell Biol.* 2:21–32.

Norbury, C., J. Blow, and P. Nurse. 1991. Regulatory phosphorylation of the p34cdc2 protein kinase in vertebrates. *EMBO J.* 10:3321–3329.

Nurse, P. 1990. Universal control mechanism regulating onset of M-phase. *Nature.* 344:503–508.

Okumura, E., T. Fukuhara, H. Yoshida, S. Hanada Si, R. Kozutsumi, M. Mori, K. Tachibana, and T. Kishimoto. 2002. Akt inhibits Myt1 in the signalling pathway that leads to meiotic G2/M-phase transition. *Nat. Cell Biol.* 4:111–116.

Parker, L.L., and H. Piwnica-Worms. 1992. Inactivation of the p34cdc2-cyclin B complex by the human WEE1 tyrosine kinase. *Science.* 257:1955–1957.

Parker, L.L., P.J. Sylvestre, M.J. Byrnes, F. Liu, and H. Piwnica-Worms. 1995. Identification of a 95-kDa WEE1-like tyrosine kinase in HeLa cells. *Proc. Natl. Acad. Sci. USA.* 92:9638–9642.

Pines, J. 1999. Four-dimensional control of the cell cycle. *Nat. Cell Biol.* 1:E73–E79.

Shibata, Y., G.K. Voeltz, and T.A. Rapoport. 2006. Rough sheets and smooth tubules. *Cell.* 126:435–439.

Shorter, J., and G. Warren. 2002. Golgi architecture and inheritance. *Annu. Rev. Cell Dev. Biol.* 18:379–420.

Solomon, M.J., T. Lee, and M.W. Kirschner. 1992. Role of phosphorylation in p34cdc2 activation: identification of an activating kinase. *Mol. Biol. Cell.* 3:13–27.

Sutterlin, C., P. Hsu, A. Mallabiabarrena, and V. Malhotra. 2002. Fragmentation and dispersal of the pericentriolar Golgi complex is required for entry into mitosis in mammalian cells. *Cell.* 109:359–369.

Takizawa, C.G., and D.O. Morgan. 2000. Control of mitosis by changes in the subcellular location of cyclin-B1-Cdk1 and Cdc25C. *Curr. Opin. Cell Biol.* 12:658–665.

Terasaki, M. 2000. Dynamics of the endoplasmic reticulum and golgi apparatus during early sea urchin development. *Mol. Biol. Cell.* 11:897–914.

Voeltz, G.K., M.M. Rolls, and T.A. Rapoport. 2002. Structural organization of the endoplasmic reticulum. *EMBO Rep.* 3:944–950.

Wells, N.J., N. Watanabe, T. Tokusumi, W. Jiang, M.A. Verdecia, and T. Hunter. 1999. The C-terminal domain of the Cdc2 inhibitory kinase Myt1 interacts with Cdc2 complexes and is required for inhibition of G(2)/M progression. *J. Cell Sci.* 112:3361–3371.

Yonemura, S., M. Itoh, A. Nagafuchi, and S. Tsukita. 1995. Cell-to-cell adherens junction formation and actin filament organization: similarities and differences between non-polarized fibroblasts and polarized epithelial cells. *J. Cell Sci.* 108:127–142.